Supplement of Biogeosciences Discuss., 12, 3943–3990, 2015
http://www.biogeosciences-discuss.net/12/3943/2015/
doi:10.5194/bgd-12-3943-2015-supplement

Biogeosciences Discussions
Open Access

Supplement of

Changes in dissolved iron deposition to the oceans driven by human activity: a 3-D global modelling study

S. Myriokefalitakis et al.
Correspondence to: S. Myriokefalitakis (stelios@chemistry.uoc.gr) and M. Kanakidou (mariak@chemistry.uoc.gr)

Table S1. Emissions used in TM4-ECPL for a) present (year 2008), b) past (year 1850) and c) future (year 2100) simulations**.** All emissions are in Tg yr^{-1}, except for NOx (Tg-N yr^{-1}), NH_3 (Tg-N yr^{-1}), SO_x (Tg-S yr^{-1}) and DMS (Tg-S yr^{-1}).

Species		**Biomass Burning**	**Anthropogenic**	**Aircrafts**	**Ships**	**Biogenic**	**Soils**	**Oceans**
ACETONE	1850	6.46E-02	4.23E-01					
	2008	4.23E+00	2.64E+00	3.03E-07		3.59E+01		
	2100	5.09E+00	2.73E+00	2.80E-07				
BC	1850	2.62E-01	1.05E+00		8.05E-04			
	2008	2.62E+00	5.39E+00	8.39E-06	1.24E-01			
	2100	3.17E+00	1.11E+00	7.32E-06	1.43E-02			
BENZENE	1850	4.83E-01	7.51E-01		8.05E-04			
	2008	4.83E+00	6.31E+00	4.90E-06	1.16E-01			
	2100	5.89E+00	2.15E+00	4.52E-06	4.80E-02			
C_2H_4	1850	6.35E-01	1.24E+00		2.21E-03			
	2008	6.35E+00	6.87E+00	3.04E-06	2.57E-01	1.75E+01		1.20E+00
	2100	7.76E+00	2.24E+00	2.80E-06	1.06E-01			
C_2H_6	1850	3.17E-01	5.93E-01		1.01E-03			
	2008	3.17E+00	2.87E+00	4.37E-06	1.50E-01	3.01E-01		8.00E-01
	2100	3.96E+00	8.09E-01	4.03E-06	6.22E-02			
C_3H_6	1850	6.26E-01	9.14E-01		2.56E-03			
	2008	6.25E+00	6.41E+00	4.64E-06	2.98E-01	1.66E+01		1.30E+00
	2100	7.68E+00	2.27E+00	4.29E-06	1.23E-01			
C_3H_8	1850	1.96E-01	2.42E-01		1.96E-01			
	2008	1.96E+00	3.47E+00	4.87E-06	4.17E-01	3.01E-02		1.00E+00
	2100	2.54E+00	1.26E+00	4.50E-06	1.73E-01			
C_4H_{10}	1850	9.07E-02	4.56E-01		6.27E-03			
	2008	9.07E-01	3.32E+01	4.01E-05	8.79E-01	6.09E-02		6.80E+00
	2100	1.11E+00	1.96E+01	3.70E-05	3.64E-01			
CH_2O	1850	5.87E-01	1.45E-01					
	2008	5.86E+00	3.39E+00	7.54E-07		4.33E+00		
	2100	7.21E+00	1.43E+00	6.97E-07				
CH_3CHO	1850	4.86E-01	3.16E-01					
	2008	4.85E+00	1.80E+00	2.07E-06		2.04E+01		
	2100	6.00E+00	5.95E-01	1.91E-06				
CH_3OH	1850	1.17E+00	6.14E-01					
	2008	1.17E+01	4.87E+00	2.90E-06		1.38E+02		
	2100	1.42E+01	2.85E+00	2.68E-06				
CO	1850	4.61E+01	6.30E+01		7.74E-03	8.37E+01		2.00E+01
	2008	4.60E+02	5.99E+02	6.55E-04	1.15E+00			

	2100	5.49E+02	2.34E+02	5.11E-04	2.29E-01			
MEK	1850	0.00E+00	0.00E+00	0.00E+00	0.00E+00			
	2008			1.04E-06		6.98E-01		
	2100			9.58E-07				
NOx	1850	7.74E-03	7.74E-03		7.74E-03			
	2008	5.48E+00	2.67E+01	1.44E-03	5.14E+00		8.00E+00	
	2100	6.39E+00	7.48E+00	1.84E-03	9.47E-01			
POA	1850	2.33E+00	4.63E+00		9.05E-04			
	2008	2.33E+01	1.39E+01	2.52E-06	1.29E-01			
	2100	2.82E+01	3.46E+00	2.20E-06	1.42E-02			
SOx	1850	1.93E-01	1.01E+00		3.60E-02			
	2008	1.93E+00	4.69E+01	1.14E-04	5.22E+00			
	2100	2.21E+00	7.70E+00	1.00E-04	5.04E-01			
TOLUENE	1850	1.42E-01	3.55E-01		5.71E-04			
	2008	1.42E+00	7.22E+00	7.36E-06	6.71E-02	1.41E+00		
	2100	1.73E+00	4.70E+00	6.80E-06	2.78E-02			
XYLENE	1850	3.71E-02	2.57E-01		1.56E-03			
	2008	3.70E-01	1.18E+01	6.69E-06	2.06E-01			
	2100	4.51E-01	7.66E+00	8.52E-02	6.18E-06			
CH_3COOH	1850	1.73E+00	1.45E+00					
	2008	1.73E+01	7.46E+00			3.25E+00		
	2100	2.08E+01	2.33E+00					
HCOOH	1850	4.33E-01	3.62E-01					
	2008	4.32E+00	1.87E+00			3.25E+00		
	2100	5.21E+00	5.83E-01					
DMS	1850	1.47E-04						
	2008	1.47E-03						1.90E+01
	2100	1.76E-03						
GLY	1850	5.87E-01						
	2008	5.86E+00						2.00E+01
	2100	7.21E+00						
NH3	1850	9.20E-01	5.40E+00					
	2008	9.20E+00	3.41E+01					8.00E+00
	2100	1.00E+01	5.15E+01					
ISOPRENE	2008					5.20E+02		1.00E+00
TERPENE	2008					1.04E+02		2.00E-04

Table S2. Aqueous-phase Fe-chemical mechanism used in the TM4-ECPL

Reactions	K_{298} ($M^{-n+1}s^{-1}$)	Ea/R (K)	References
$Fe^{2+} + H_2O_2 \rightarrow Fe^{3+} + OH + ^{-}OH$	5.24×10^{1}	5050	Kremer, 2003
$Fe^{2+} + O_2^{-\cdot} + 2H^{+} \rightarrow Fe^{3+} + H_2O_2$	1.00×10^{7}	5050	Rush and Bielski, 1985
$Fe^{2+} + HO_2 + H^{+} \rightarrow Fe^{3+} + H_2O_2$	1.20×10^{6}	5050	Jayson et al., 1973b
$Fe^{2+} + OH \rightarrow Fe(OH)^{2+}$	4.60×10^{8}	1100	Christensen and Sehested, 1981
$Fe^{2+} + NO_3 \rightarrow Fe^{3+} + NO_3^{-}$	8.00×10^{6}		Pikaev et al., 1974
$Fe^{2+} + NO_2 + H+ \rightarrow Fe^{3+} + HONO$	3.10×10^{4}		Epstein et al., 1982
$Fe^{2+} + O_3 (+ H_2O) \rightarrow {}^{*}Fe(OH)^{2+} + OH + O_2$	8.20×10^{5}		Logager et al., 1992
$Fe^{3+} + hv (+ H_2O) \rightarrow Fe^{2+} + OH + H^{+}$	$6.41 \text{ x } 10^{-6}$		Benkelberg and Warneck, 1995
$Fe(OH)^{2+} + hv \rightarrow Fe^{2+} + OH$	4.51×10^{-3}		Benkelberg and Warneck, 1995
$Fe(OH)_2^{+} + hv \rightarrow Fe^{2+} + OH + ^{-}OH$	5.77×10^{-3}		Benkelberg et al., 1991
$Fe(OH)^{2+} + O_2^{-} \rightarrow Fe^{2+} + O_2 + ^{-}OH$	1.50×10^{8}		Rush and Bielski, 1985
$Fe(OH)^{2+} + HO_2 \rightarrow Fe^{2+} + O_2 + H_2O$	1.30×10^{5}		Ziajka et al., 1994
$Fe^{3+} + SO_4^{2-} \rightarrow Fe(SO_4)^{+}$	3.20×10^{3}		Jayson et al., 1973b
$Fe(SO_4)^{+} \rightarrow Fe^{3+} + SO_4^{2-}$	2.70×10^{1}		Jayson et al., 1973b
$Fe(SO_4)^{+} + hv \rightarrow Fe^{2+} + SO_4^{-}$	6.43×10^{-3}		Lin et al., 2014
$Fe^{3+} + C_2O_4^{2-} \rightarrow Fe(C_2O_4)^{+}$	7.50×10^{6}		Lin et al., 2014
$Fe(C_2O_4)^{+} \rightarrow Fe^{3+} + C_2O_4^{2-}$	3.00×10^{-3}		Lin et al., 2014
$Fe(C_2O_4)^{+} + C_2O_4^{2-} \rightarrow Fe(C_2O_4)_2^{-}$	1.89×10^{4}		Lin et al., 2014
$Fe(C_2O_4)_2^{-} \rightarrow Fe(C_2O_4)^{+} + C_2O_4^{2-}$	3.30×10^{-3}		Lin et al., 2014
$Fe(C_2O_4)^{+} + O_2^{-} \rightarrow Fe(C_2O_4) + O_2$	1.00×10^{6}		Sedlak and Hoigne, 1993
$Fe(C_2O_4)^{+} + HO_2 \rightarrow Fe(C_2O_4) + O_2 + H^{+}$	1.20×10^{5}		Sedlak and Hoigne, 1993
$Fe(C_2O_4)_2^{-} + O_2^{-} \rightarrow Fe(C_2O_4)_2^{2-} + O_2$	1.00×10^{6}		Sedlak and Hoigne, 1993
$Fe(C_2O_4)_2^{-} + HO_2 \rightarrow Fe(C_2O_4)_2^{2-} + O_2 + H^{+}$	1.20×10^{5}		Sedlak and Hoigne, 1993
$Fe(C_2O_4) + H_2O_2 \rightarrow Fe(C_2O_4)^{+} + OH + ^{-}OH$	5.24×10^{4}		Sedlak and Hoigne, 1993
$Fe(C_2O_4)_2^{-} + hv (+ O_2) \rightarrow Fe^{+2} + C_2O_4^{2-} + 2CO_2 + O_2^{-}$	2.47×10^{-2}		Lin et al., 2014
Equilibrium	Keq (mol kg^{-1})		
$Fe^{3+} + H_2O \leftrightarrow Fe(OH)^{2+} + H^{+}$	1.10×10^{-4}		Ervens et al., 2003
$Fe(OH)^{2+} + H_2O \leftrightarrow Fe(OH)_2^{+} + H^{+}$	1.40×10^{-7}		Ervens et al., 2003

Table S3. Number of measurements (N), mean correlation coefficient (*r*), normalised mean bias (*NMB*), normalised mean error (*NME*) and root mean square error (*RMSE*) values calculated for total Iron (TFe) and dissolved Iron (DFe) as presented in Fig 5..

Figure	TM4-ECPL	**N**	**R**	**NMB (%)**	**NME (%)**	**RMSE (ng-Fe/m^3)**
Fig. 5a	**TFe**	412	0.06	2406	147	6196
Fig. 5b	**DFe**	412	0.06	67	84	29
Fig. 5c	**TFe**	452	0.4	16	89	760

$$R = \left[\frac{\frac{1}{N}\sum_{i=1}^{N}\left(O_i - \overline{O}\right)\left(P_i - \overline{P}\right)}{\sigma_O \sigma_P} \right] \quad \text{(eq. S1)}$$

$$NMB = \frac{\sum_{i=1}^{N}\left(M_i - O_i\right)}{\sum_{i=1}^{N} O_i} \times 100 \quad \text{(eq. S2)}$$

$$RMSE = \sqrt{\frac{1}{N}\sum_{i=1}^{N}\left(P_i - O_i\right)^2} \quad \text{(eq. S3)}$$

$$NME = \frac{\sum_{i=1}^{N}\left|M_i - O_i\right|}{\sum_{i=1}^{N} O_i} \times 100 \quad \text{(eq. S4)}$$

Figure S1. Annual mean surface concentrations of a) dust (in μg m^{-3}) and TFe in iron-containing minerals, b) Kaolinite, c) Illite, d) Smectite, e) Hematite, f) Feldspars g) in anthropogenic aerosols (from fossil fuel including shipping emissions) and h) in biomass burning aerosols (in μg-Fe m^{-3}) as calculated by TM4-ECPL for the present atmosphere.

a)

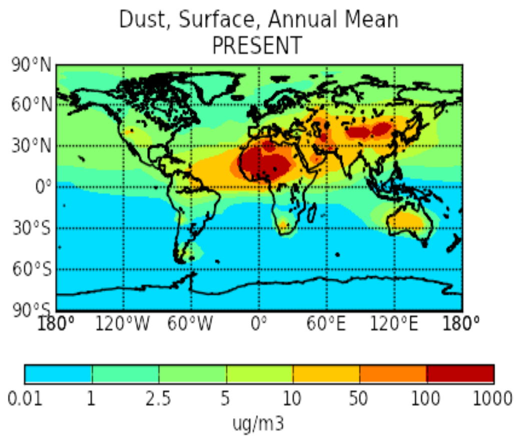

b)

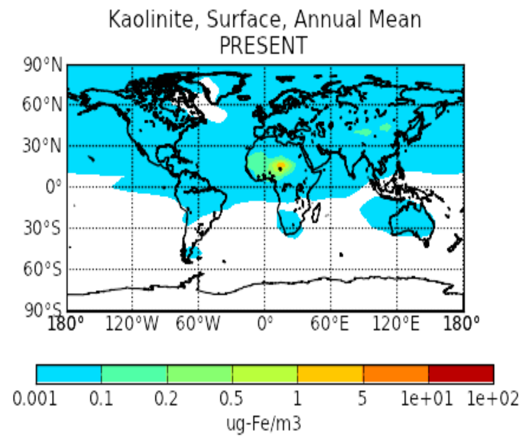

c)

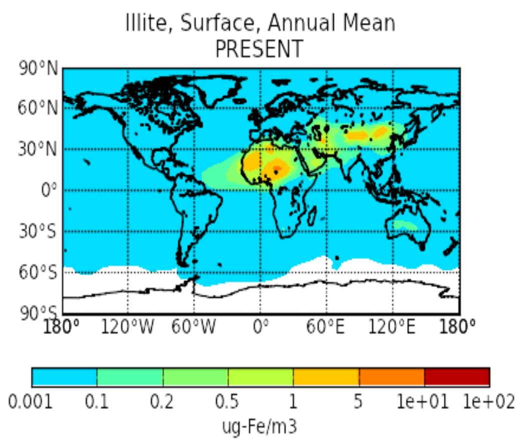

d)

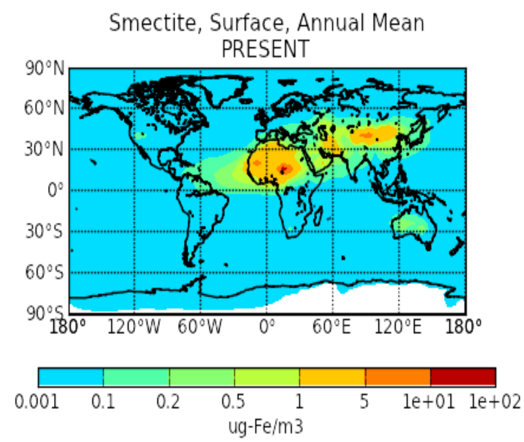

e)

f)

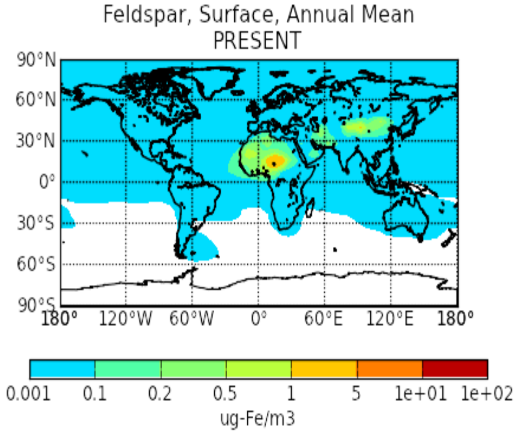
Feldspar, Surface, Annual Mean
PRESENT
90°N
60°N
30°N
0°
30°S
60°S
90°S
180°
120°W
60°W
0°
60°E
120°E
180°
0.001
0.1
0.2
0.5
1
5
1e+01
1e+02
ug-Fe/m3

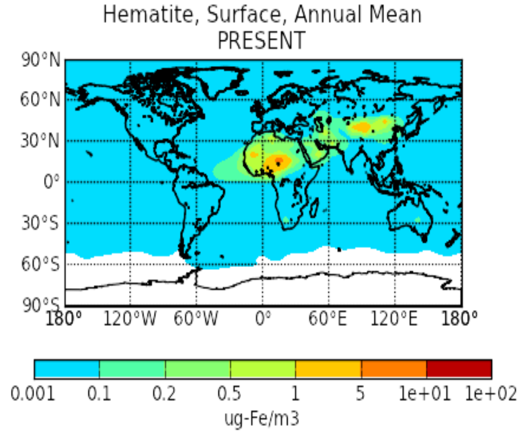
Hematite, Surface, Annual Mean
PRESENT
90°N
60°N
30°N
0°
30°S
60°S
90°S
180°
120°W
60°W
0°
60°E
120°E
180°
0.001
0.1
0.2
0.5
1
5
1e+01
1e+02
ug-Fe/m3

g)

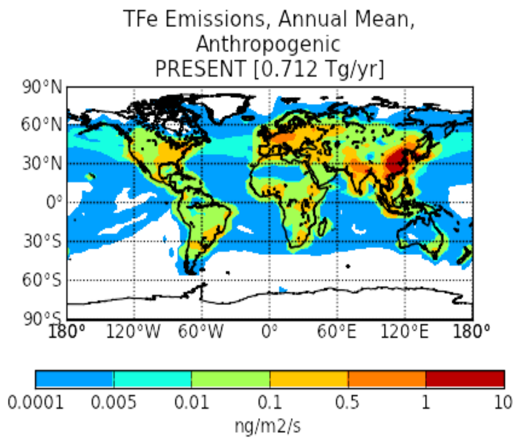
TFe Emissions, Annual Mean,
Anthropogenic
PRESENT [0.712 Tg/yr]
90°N
60°N
30°N
0°
30°S
60°S
90°S
180°
120°W
60°W
0°
60°E
120°E
180°
0.0001
0.005
0.01
0.1
0.5
1
10
ng/m2/s

h)

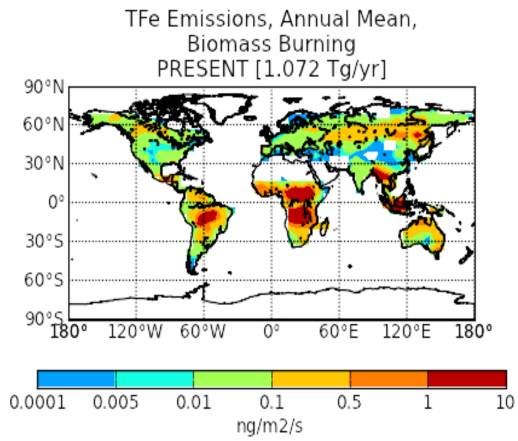
TFe Emissions, Annual Mean,
Biomass Burning
PRESENT [1.072 Tg/yr]
90°N
60°N
30°N
0°
30°S
60°S
90°S
180°
120°W
60°W
0°
60°E
120°E
180°
0.0001
0.005
0.01
0.1
0.5
1
10
ng/m2/s

Figure S2. Calculated annual mean concentrations for the present atmosphere for the dissolved Fe fractions in ng-Fe m^{-3}: Fe(III) (a,b) and Fe(II) (c,d) for surface (left panels: a,c) and zonal mean (b,d).

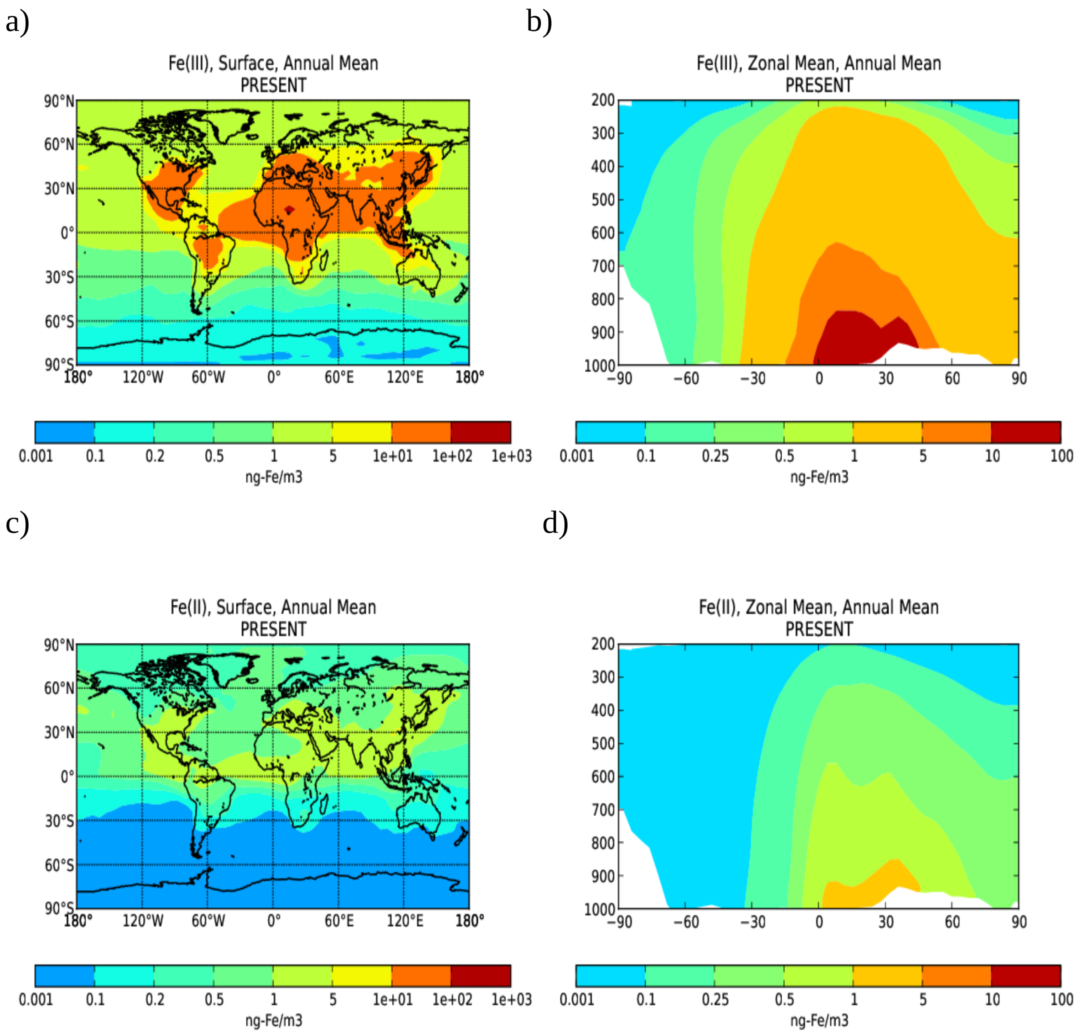

Figure S3. Absolute differences (in µg m^{-3}) of surface concentrations calculated by TM4-ECPL using the emissions of PAST (left panels: a, c, e, g) and FUTURE (right panels: b, d, f, h) from those calculated using the present-day emission scenario (PRESENT) for a, b) SO_4^{2-}; c, d) NO_3^-; e, f) NH_4^+ and g, h) for OXL.

a)

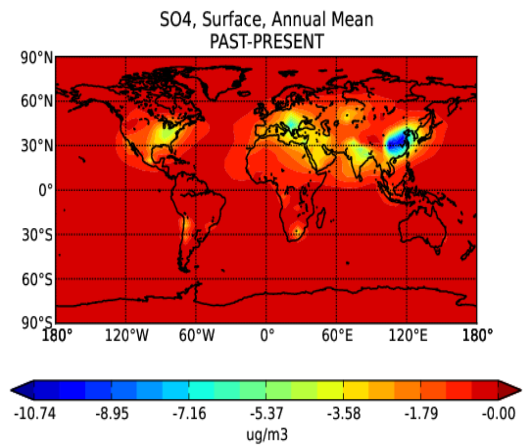

b)

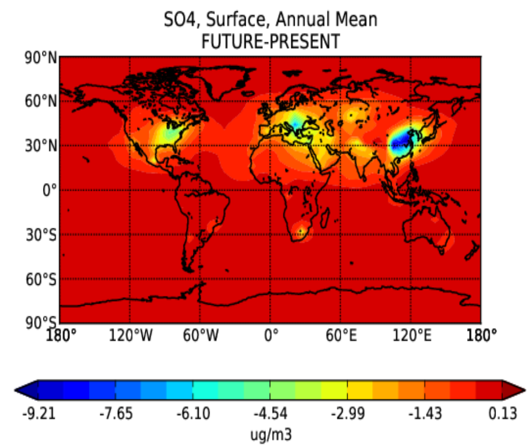

c)

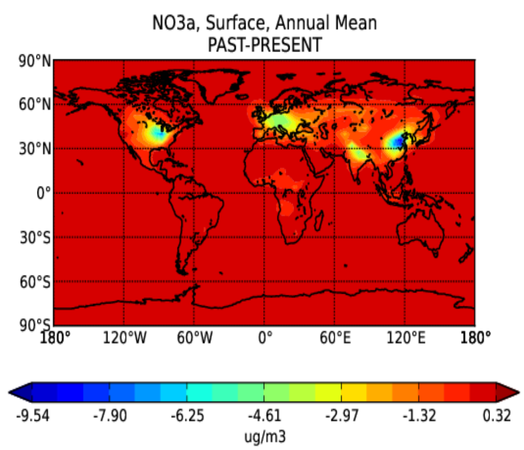

d)

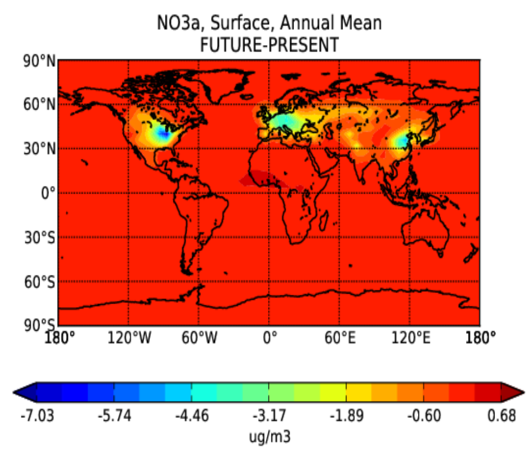

e)

f)

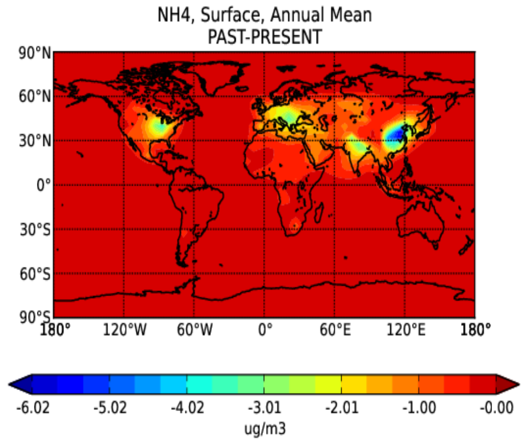
NH4, Surface, Annual Mean
PAST-PRESENT
90°N
60°N
30°N
0°
30°S
60°S
90°S
180°
120°W
60°W
0°
60°E
120°E
180°
-6.02
-5.02
-4.02
-3.01
-2.01
-1.00
-0.00
ug/m3

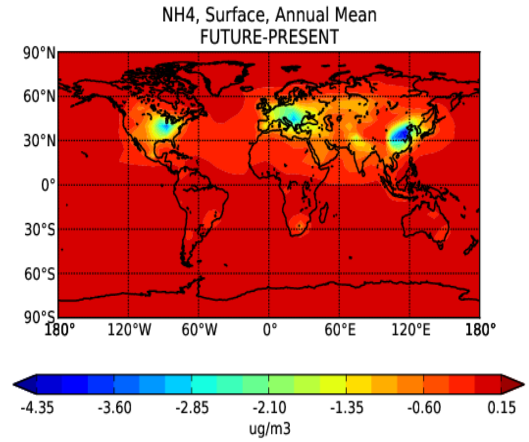
NH4, Surface, Annual Mean
FUTURE-PRESENT
90°N
60°N
30°N
0°
30°S
60°S
90°S
180°
120°W
60°W
0°
60°E
120°E
180°
-4.35
-3.60
-2.85
-2.10
-1.35
-0.60
0.15
ug/m3

g)

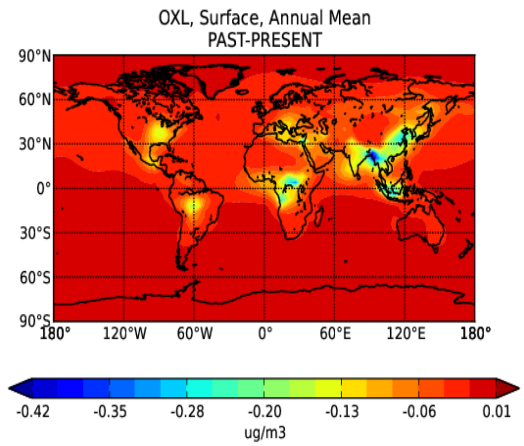
OXL, Surface, Annual Mean
PAST-PRESENT
90°N
60°N
30°N
0°
30°S
60°S
90°S
180°
120°W
60°W
0°
60°E
120°E
180°
-0.42
-0.35
-0.28
-0.20
-0.13
-0.06
0.01
ug/m3

h)

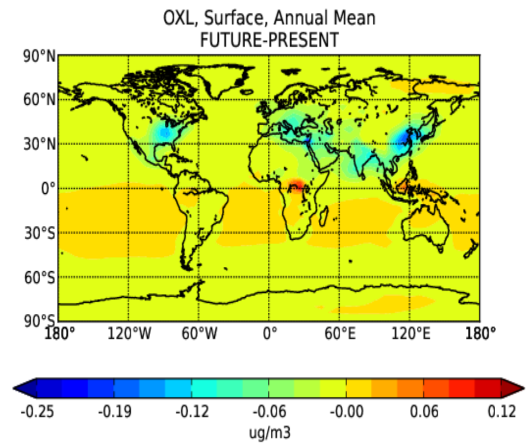
OXL, Surface, Annual Mean
FUTURE-PRESENT
90°N
60°N
30°N
0°
30°S
60°S
90°S
180°
120°W
60°W
0°
60°E
120°E
180°
-0.25
-0.19
-0.12
-0.06
-0.00
0.06
0.12
ug/m3

Figure S4. Percentage changes (%) in pH calculated by TM4-ECPL using the emissions of PAST (left panels: a, c) and FUTURE (right panels: b, d) simulations from those calculated using the present-day emission scenario (PRESENT) for surface aerosol water (a,b) and cloud water (c,d) at 500hPa.

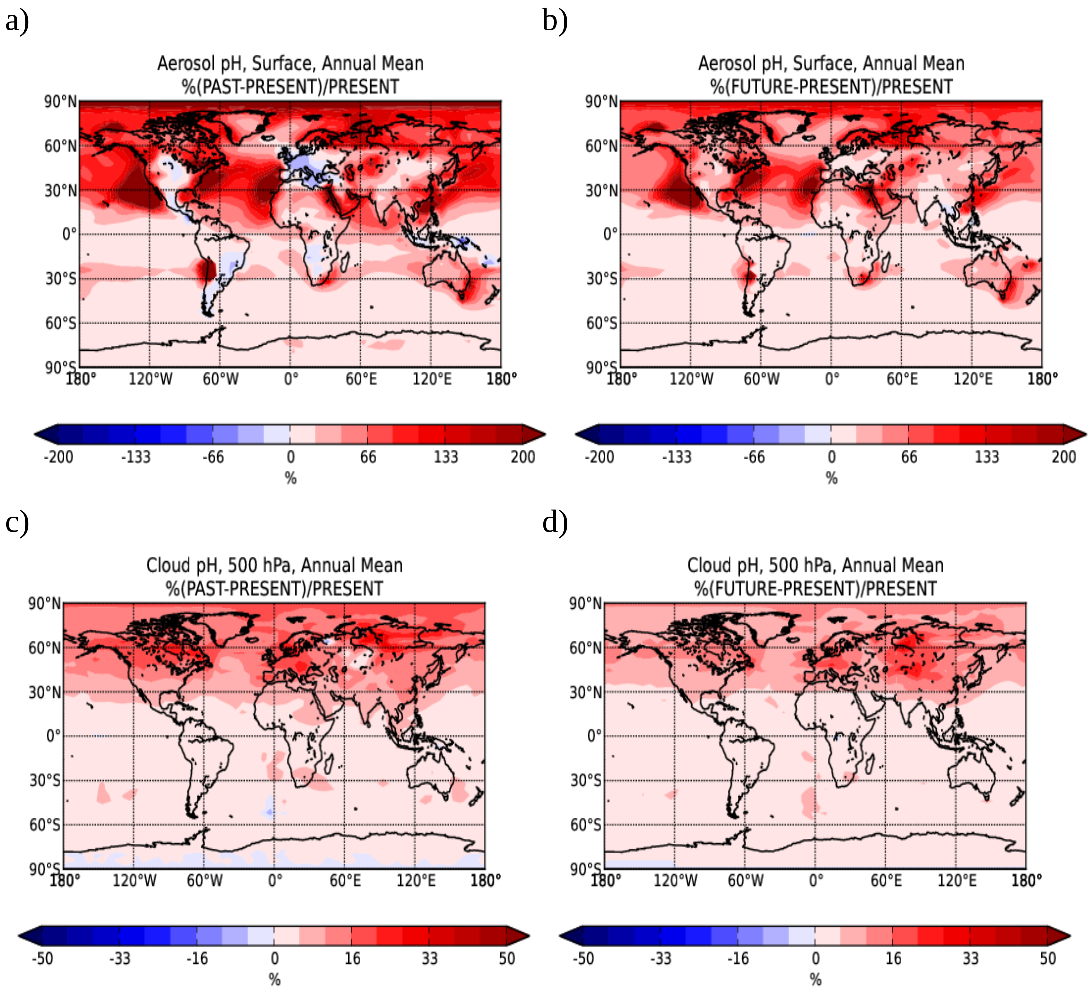

Figure S5. The surface percentage differences of PAST (left panels: a,c) and FUTURE (right panels: b,d) simulations from the PRESENT day simulation for a,b) Proton/Total Mineral Dissolution and c,d) Ligand/Total Mineral Dissolution.

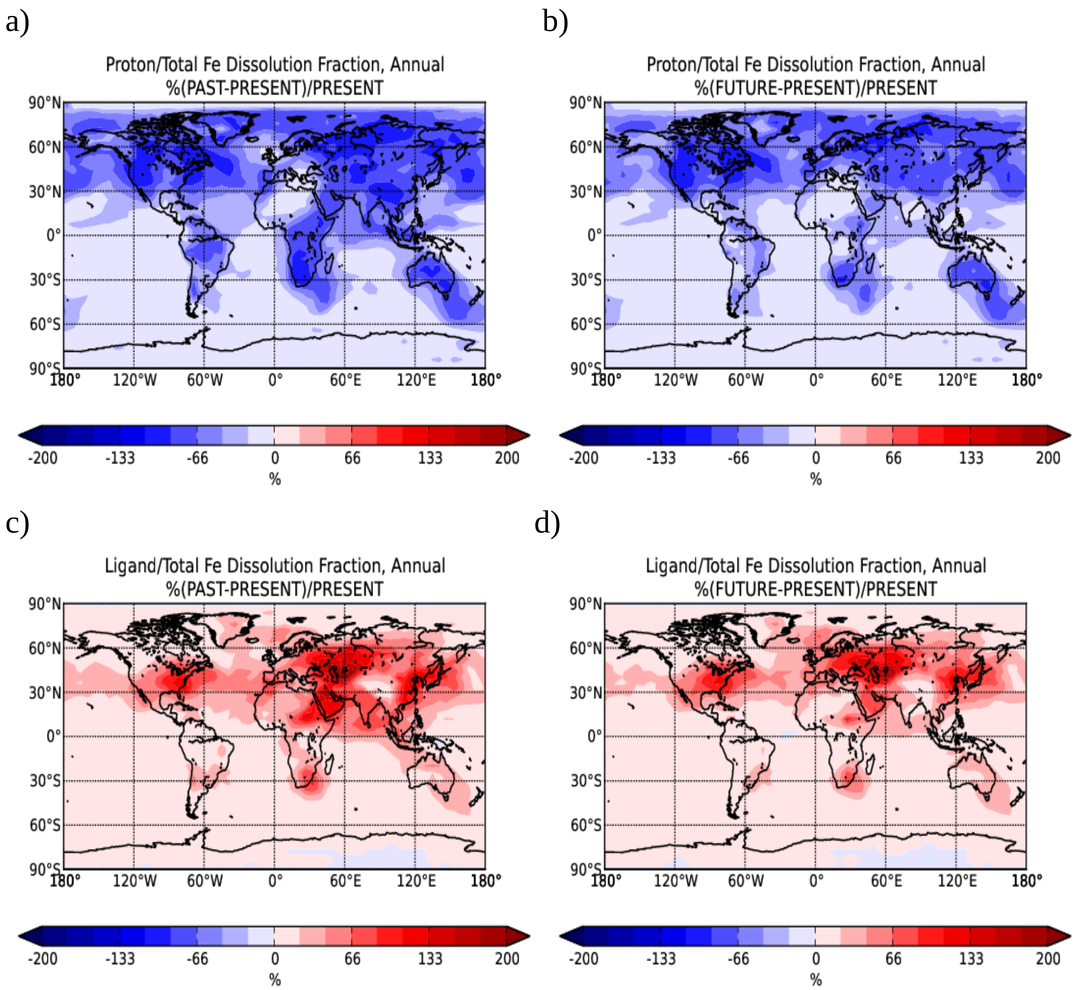

Figure S7. The surface percentage differences (%) of PAST (left panels: a,c) and FUTURE (right panels: b, d) simulations from the PRESENT day simulation for a,b) Fe(II)/DFe and c, d) Fe(III)/DFe, as calculated by TM4-ECPL.

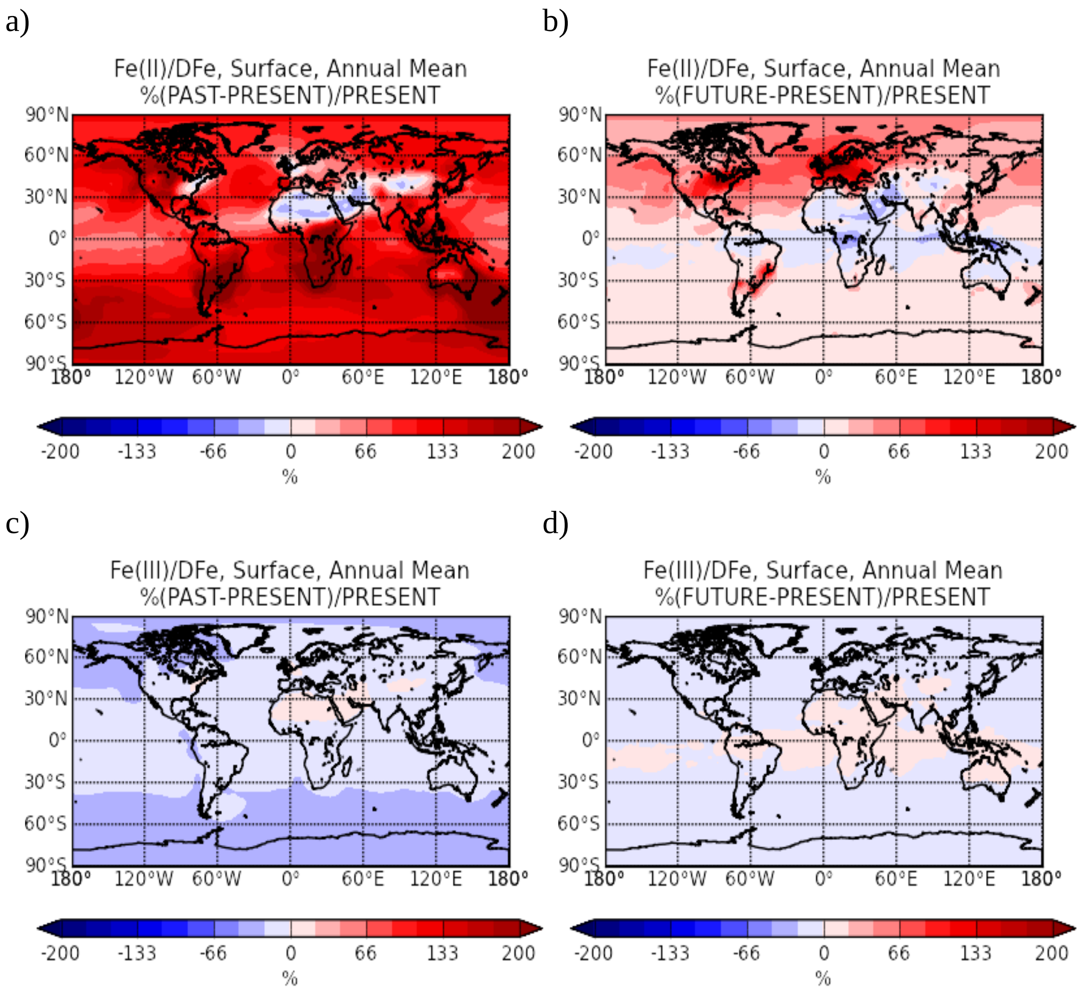

Figure S8. The percentage differences (%) of PAST (left panels: a,c) and FUTURE simulations (right panels: b,d) from the PRESENT simulation for a,b) DFe deposition and c,d) Iron Solubility (SFe), as calculated by TM4-ECPL.

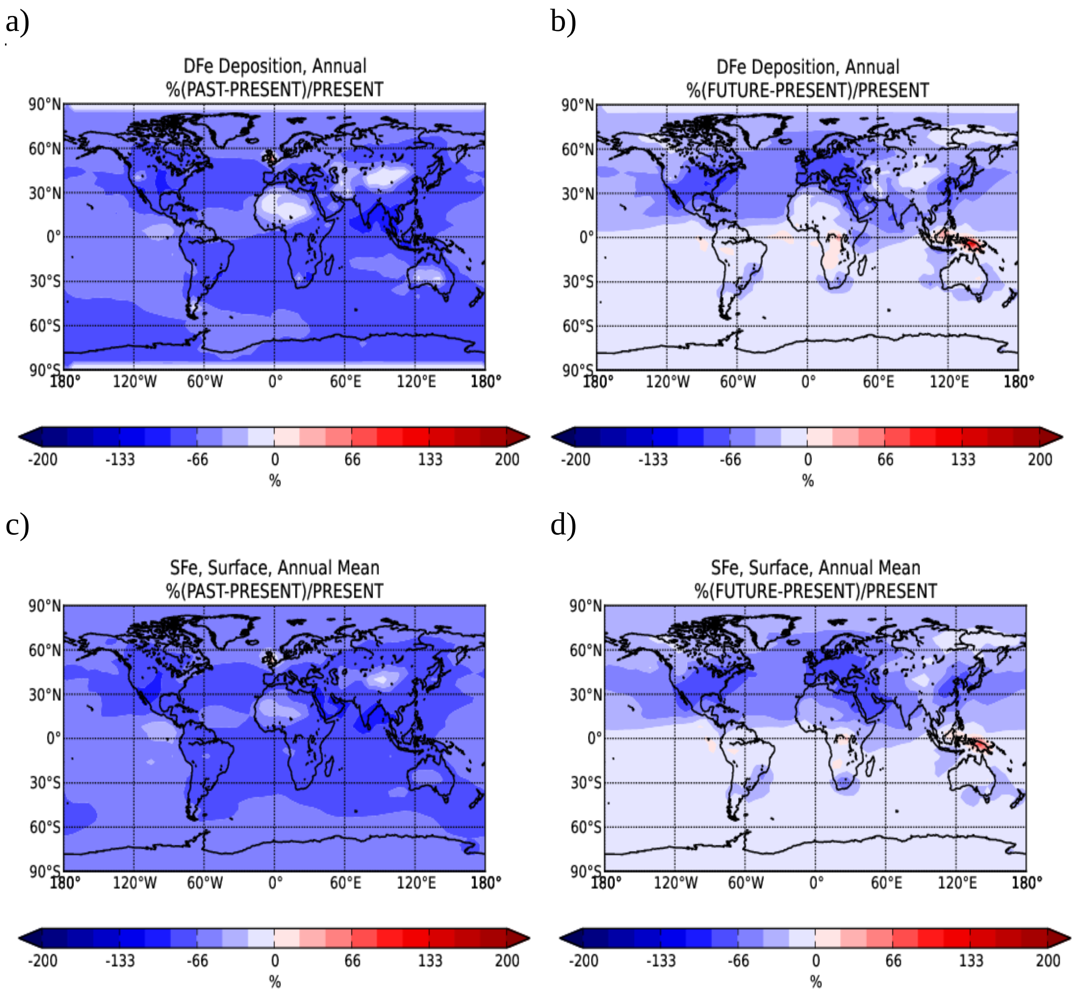

Figure S9. The percentage iron dissolution (SFe) predicted from the chemical scheme used for this study for dust concentrations 1 mg L^{-1} and pH values of 1.5, 4.5 and 8.5 for OXL concentrations of a) 0 µM, b) 4.5 µM and c) 8 µM.

a)

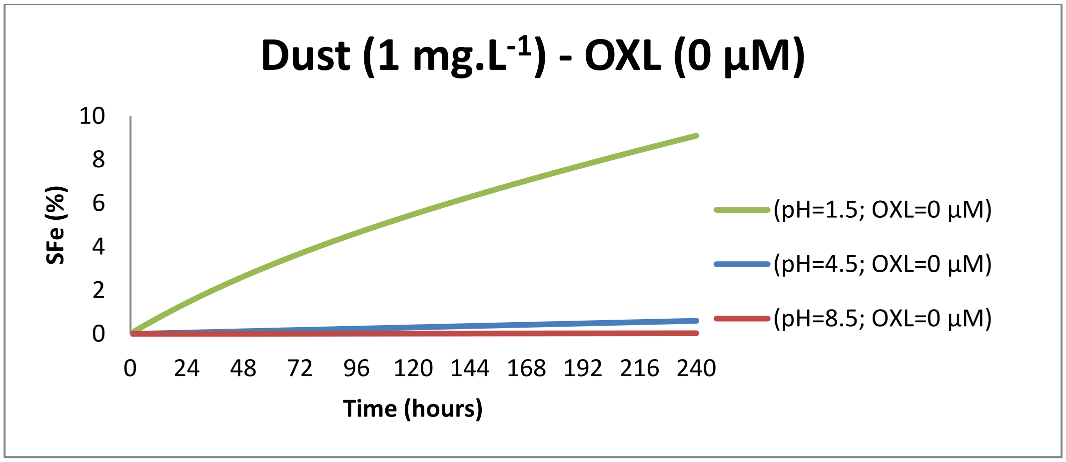

b)

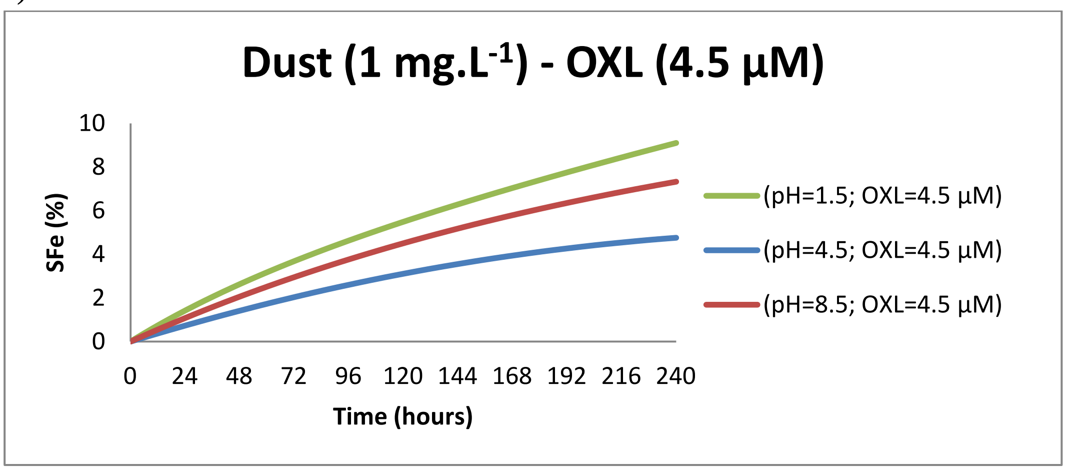

c)

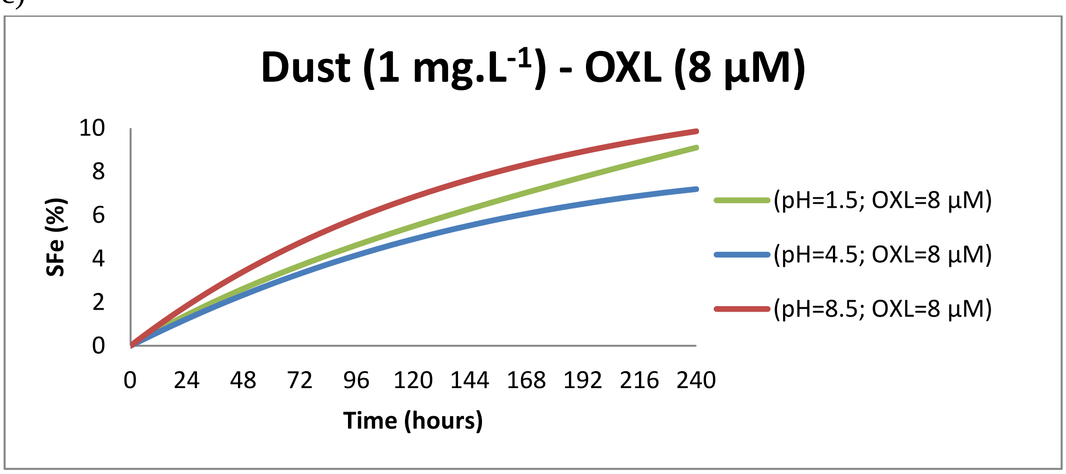

Figure S10. Map of the deposition regions (2-5) (red colour) as adopted by Baker et al. (2013) and used for the calculations of Fig. 7.

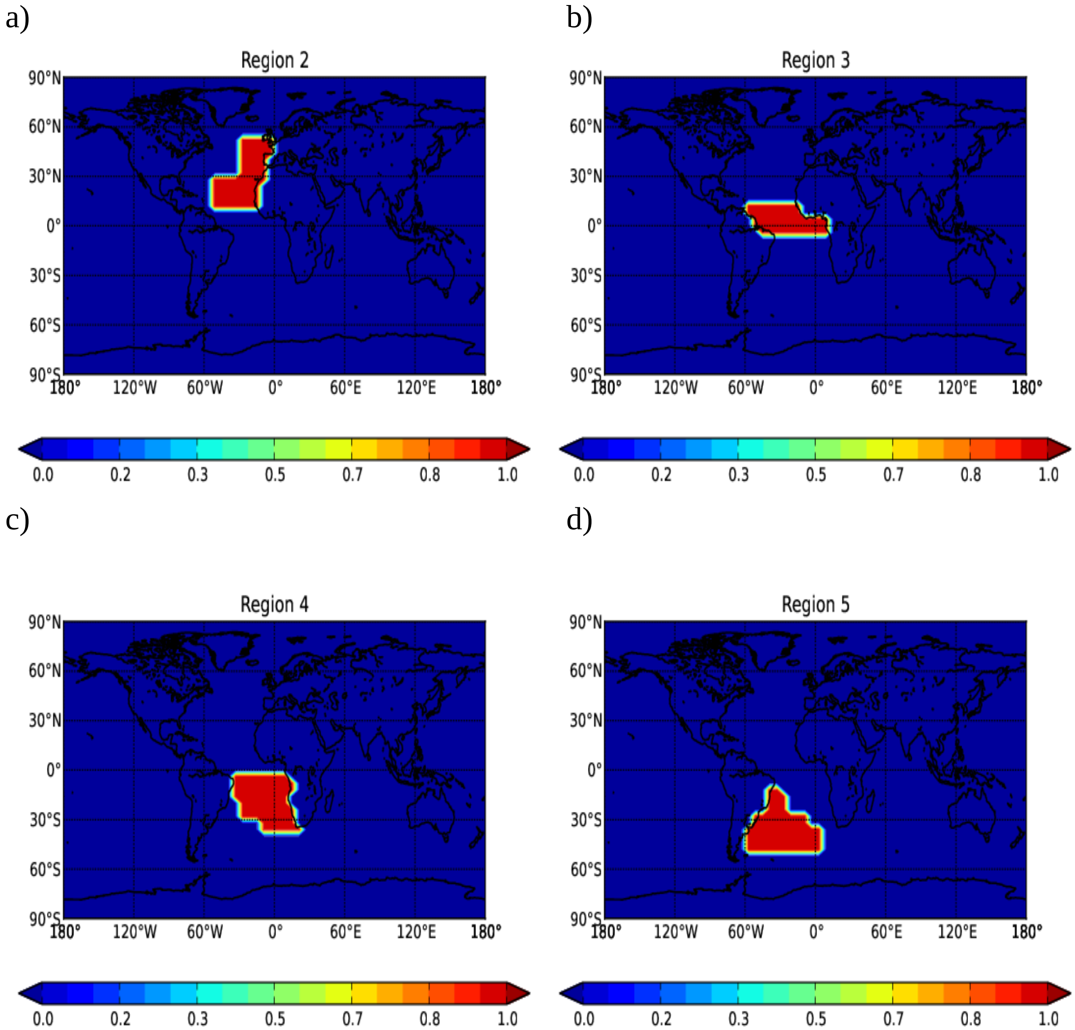

References

Benkelberg, H. J. and Warneck, P.: Photodecomposition of iron(III) hydroxo and sulfato complexes in aqueous solutions: Wavelength dependence of pH and SO −4 quantum yields, J. Phys. Chem., 99, 5214–5221, 1995.

Epstein, I. R., Kustin, K., and Simoyi, R. H.: Nitrous acid decomposition catalyzed by an iron(II) complex: Tris(3,4,7,8-tetramethyl-1,10-phenanthroline)iron(II)1 , J. Am. Chem. Soc., 104, 712–717, 1982.

Ervens, B., George, C., Williams, J. E., Buxton, G. V., Salmon, G. A., Bydde,r M., Wilkinson, F., Dentener, F., Mirabel, P., Wolk, R. and Herrmann, H. : CAPRAM 2.4 (MODAC mechanism): An extended and condensed tropospheric aqueous phase mechanism and its application, J. Geophys. Res., 108(D14), 4426, doi:10.1029/2002JD002202, 2003.

Jayson, G. G., Parson, B. J., and Swallow, A. J.: Oxidation of ferrous ions by perhydroxyl radicals, J. Chem. Soc. Faraday Trans., 69, 236–242, 1973.

Kremer, M. L.: The Fenton reaction, Dependence of the rate on pH, J. Phys. Chem. A, 107, 1734–1741, 2003.

Lin, G., Sillman, S., Penner, J. E. and Ito, A.: Global modeling of SOA: The use of different mechanisms for aqueous-phase formation, Atmos. Chem. Phys., 14, 5451–5475, doi:10.5194/acp-14-5451-2014, 2014.

Logager, T., Holcman, J., Sehested, K., and Pedersen, T.: Oxidation of ferrous ions by ozone in acidic solution, Inorg. Chem., 31, 3523–3529, 1992.

Pikaev, A. K., Sibirskaya, G. K., Shirshov, E. M., Glazunov, P. Y., and Spitsyn, V. I.: Pulsed radiolysis of concentrated aqueous solutions of nitric acid, Dokl. Phys. Chem., Proc. Acad. Sci. USSR, 215, 328–331, 1974.

Rush, J. D. and Bielski, B. H. J.: Pulse radiolytic studies of the reactions of HO2/O2 with Fe(II)/Fe(III) ions, The reactivity of HO2/O2 with ferric ions and its implication on the occurrence of the Haber-Weiss reaction, J. Phys. Chem., 89, 5062–5066, doi:10.1021/j100269a035, 1985.

Rush, J. D. and Bielski, B. H. J.: Pulse radiolytic studies of thereactions of HO2/O2 with Fe(II)/Fe(III) ions, The reactivity of HO2/O2 with ferric ions and its implication on the occurrence of the Haber-Weiss reaction, J. Phys. Chem., 89, 5062–5066, doi:10.1021/j100269a035, 1985.

Sedlak, D. L. and Hoigne, J.: The role of copper and oxalate in the´ redox cycling of iron in atmospheric waters, Atmos. Environ., 27A, 2173–2185, 1993.